Asian Journal of Chemistry; Vol. 27, No. 7 (2015), 2603-2607

ASIAN JOURNAL OF CHEMISTRY

http://dx.doi.org/10.14233/ajchem.2015.18429

Synthesis of $KLa(WO_4)_2$:Ho^{3+}/Yb^{3+} Phosphors *via* Microwave-Assisted Sol-Gel Route and their Upconversion Photoluminescence Properties

CHANG SUNG LIM

Department of Advanced Materials Science and Engineering, Hanseo University, Seosan 356-706, Republic of Korea

Corresponding author: Tel/Fax: +82 41 6601445; E-mail: cslim@hanseo.ac.kr

Received: 18 July 2014; *Accepted*: 29 November 2014; *Published online*: 30 March 2015; AJC-17088

Double tungstate $KLa_{1-x}(WO_4)_2$:Ho^{3+}/Yb^{3+} phosphors with doping concentrations of Ho^{3+} and Yb^{3+} ($x = Ho^{3+} + Yb^{3+}$, $Ho^{3+} = 0.05, 0.1, 0.2$ and $Yb^{3+} = 0.2, 0.45$) were successfully synthesized *via* the microwave-assisted sol-gel route and the upconversion of their photoluminescence properties was investigated. Well-crystallized particles, formed after heat-treatment at 900 °C for 16 h, showed a fine and homogeneous morphology with particle sizes of 2-5 μm. Under excitation at 980 nm, the upconversion intensity of $KLa_{0.5}(MoO_4)_4$:$Ho_{0.05}Yb_{0.45}$ phosphor exhibited a strong 550 nm emission band in the green region and a very strong 655 nm emission band in the red region. The Raman spectra of the particles indicated the presence of strong peaks at higher frequencies and weak peaks at lower frequencies induced by the disorder of the $[WO_4]^{2-}$ groups with the incorporation of the Ho^{3+} and Yb^{3+} elements into the crystal lattice or by a new phase formation.

Keywords: Upconversion photoluminescence, Double tungstates, Microwave-assisteded sol-gel, Raman spectroscopy.

INTRODUCTION

Upconversion (UC) materials have attracted consideration attention because of their unique optical, spectral and chemical properties induced by the special configurations and energy band gaps of the rare earth ions. These materials have been widely applied in the fields, such as lighting sources, display terminals and biological detectors[1,2]. Recently, the synthesis and the luminescence properties of upconversion particles have attracted considerable interest since they are considered as potentially active components in new optoelectronic devices and luminescent labels for imaging and biodetection assays, which overcome the current limitations in traditional photoluminescence materials[3]. Most of $MR(WO_4)_2$ (M = Li, Na, K; R = La, Gd, Y) possess the tetragonal scheelite structure with the space group $I4_{1/a}$ and belong to the family of double tungstates compounds. It is possible for the trivalent rare earth ions in the disordered tetragonal-phase to be partially substituted by Ho^{3+} and Yb^{3+} ions, these ions are effectively doped into the crystal lattices of the tetragonal phase due to the similar radii of the trivalent rare earth ions in R^{3+}, this results in high red emitting efficiency and superior thermal and chemical stability. In these compounds, W^{6+} is coordinated by four O^{2-} at a tetrahedral site, which makes $[WO_4]^{2-}$ relatively stable. R^{3+} and M^{+} are randomly distributed over the same cationic sublattice and they are coordinated by eight O^{2-} from near four $[WO_4]^{2-}$ with a symmetry S_4 without an inversion center[4-6]. The $[WO_4]^{2-}$ group has strong absorption in the near ultraviolet region, so that energy transfers process from $[WO_4]^{2-}$ group to rare earth ions can easily occur, which can greatly enhance the external quantum efficiency of rare earth ions doped materials. Among rare earth ions, the Ho^{3+} ion is suitable for converting infrared to visible light through the upconversion process due to its appropriate electronic energy level configuration. The co-doped Yb^{3+} ion and Ho^{3+} ion can remarkably enhance the upconversion efficiency for the shift from infrared to visible light due to the efficiency of the energy transfer from Yb^{3+} to Ho^{3+}. The Yb^{3+} ion, as a sensitizer, can be effectively excited by an incident light source energy. This energy is transferred to the activator from which radiation can be emitted. The Ho^{3+} ion activator is the luminescence center of the upconversion particles, while the sensitizer enhances the upconversion luminescence efficiency[7-9].

Several processes have been developed to prepare these rare earth doped double tungsates, including solid-state reactions[4,10-12], the hydrothermal method[6,13-15], the sol-gel method[16], the solvothermal method[17], the Pechini method[18,19] and the combustion method[20,21]. Compared with the usual methods, microwave synthesis has the advantages of a very short reaction time, small-size particles, narrow particle size distribution and high purity of final polycrystalline samples. Microwave heating is delivered to the material surface by radiant and/or convection heating, which is transferred to the bulk of the material *via* conduction[21]. A cyclic microwave-

assisted sol-gel process is a cost-effective method that provides high homogeneity and is easy to scale-up and it is emerging as a viable alternative approach for the quick synthesis of high-quality luminescent materials. However, the synthesis of $KLa(WO_4)_2$: Ho^{3+}/Yb^3 phosphors *via* the microwave-assisted sol-gel route has not been reported.

In this study, $KLa_{1-x}(WO_4)_4$:Ho^{3+}/Yb^{3+} phosphors with doping concentrations of Ho^{3+} and Yb^{3+} (x = Ho^{3+} + Yb^{3+}, Ho^{3+} = 0.05, 0.1, 0.2 and Yb^{3+} = 0.2, 0.45) phosphors were prepared *via* the cyclic microwave-assisted sol-gel route followed by heat treatment. The synthesized particles were characterized by X-ray diffraction (XRD), scanning electron microscopy (SEM) and energy-dispersive X-ray spectroscopy (EDS). The optical properties were examined comparatively using photoluminescence (PL) emission and Raman spectroscopy.

EXPERIMENTAL

Appropriate stoichiometric amounts of KNO_3 (99 %, Sigma-Aldrich, USA), $La(NO_3)_3·6H_2O$ (99 %, Sigma-Aldrich, USA), $(NH_4)_6W_{12}O_{39}·xH_2O$ (99 %, Alfa Aesar, USA), $Ho(NO_3)_3·5H_2O$ (99.9 %, Sigma-Aldrich, USA), $Yb(NO_3)_3·5H_2O$ (99.9 %, Sigma-Aldrich, USA), citric acid (99.5 %, Daejung Chemicals, Korea), NH_4OH (A.R.), ethylene glycol (A.R.) and distilled water were used to prepare $KLa(WO_4)_2$, $KLa_{0.8}(WO_4)_2$:$Ho_{0.2}$, $KLa_{0.7}(WO_4)_2$:$Ho_{0.1}Yb_{0.2}$ and $KLa_{0.5}(WO_4)_2$: $Ho_{0.05}Yb_{0.45}$ compounds with doping concentrations of Ho^{3+} and Yb^{3+} (Ho^{3+} = 0.05, 0.1, 0.2 and Yb^{3+} = 0.2, 0.45). To prepare $KLa(WO_4)_2$, 0.4 mol % KNO_3 and 0.4 mol % $(NH_4)_6W_{12}O_{39}·xH_2O$ were dissolved in 20 mL of ethylene glycol and 80 mL of 5 M NH_4OH under vigorous stirring and heating. Subsequently, 0.4 mol % $La(NO_3)_3·6H_2O$ and citric acid (with a molar ratio of citric acid to total metal ions of 2:1) were dissolved in 100 mL of distilled water under vigorous stirring and heating. Then, the solutions were mixed together under vigorous stirring and heating at 80-100 °C. At the end, highly transparent solutions were obtained and adjusted to pH = 7-8 by the addition of 8 M NH_4OH or citric acid. In order to prepare $KLa_{0.8}(WO_4)_2$:$Ho_{0.2}$, the mixture of 0.32 mol % $La(NO_3)_3·6H_2O$ with 0.08 mol % $Ho(NO_3)_3·5H_2O$ was used for the creation of the rare earth solution. In order to prepare $KLa_{0.7}(WO_4)_2$:$Ho_{0.1}Yb_{0.2}$, the mixture of 0.28 mol % $La(NO_3)_3·6H_2O$ with 0.04 mol % $Ho(NO_3)_3·5H_2O$ and 0.08 mol % $Yb(NO_3)_3·5H_2O$ was used for the creation of the rare earth solution. In order to prepare $KLa_{0.5}(WO_4)_2$:$Ho_{0.05}Yb_{0.45}$, the rare earth containing solution was generated using 0.2 mol % $La(NO_3)_3·6H_2O$ with 0.02 mol % $Ho(NO_3)_3·5H_2O$ and 0.18 mol % $Yb(NO_3)_3·5H_2O$.

The transparent solutions were placed into a microwave oven operating at a frequency of 2.45 GHz with a maximum output-power of 1250 W for 0.5 h. The working cycle of the microwave reaction was controlled precisely using a regime of 40 s on and 20 s off for 15 min, followed by further treatment of 30 s on and 30 s off for 15 min. The ethylene glycol was evaporated slowly at its boiling point. Ethylene glycol is a polar solvent at its boiling point of 197 °C, this solvent is a good candidate for the microwave process. If ethylene glycol is used as the solvent, the reactions proceed at the boiling point temperature. When microwave radiation is supplied to the ethylene-glycol-based solution, the components dissolved in the ethylene glycol can couple. The charged particles vibrate in the electric field interdependently when a large amount of microwave radiation is supplied to the ethylene glycol. The samples were treated with ultrasonic radiation for 10 min to produce a light yellow transparent sol. After this, the light yellow transparent sols were dried at 120 °C in a dry oven to obtain black dried gels. The black dried gels were grinded and heat-treated at 900 °C for 16 h with 100 °C intervals between 600-900 °C. Finally, white particles were obtained for $KLa(MoO_4)_2$ and pink particles for $KLa_{0.8}(WO_4)_2$:$Ho_{0.2}$, $KLa_{0.7}(WO_4)_2$:$Ho_{0.1}Yb_{0.2}$ and $KLa_{0.5}(WO_4)_2$: $Ho_{0.05}Yb_{0.45}$ compositions.

The phase composition of the synthesized particles was identified using XRD (D/MAX 2200, Rigaku, Japan). The microstructure and surface morphology of the $KLa(MoO_4)_2$, $KLa_{0.8}(WO_4)_2$:$Ho_{0.2}$, $KLa_{0.7}(WO_4)_2$:$Ho_{0.1}Yb_{0.2}$ and $KLa_{0.5}(WO_4)_2$:$Ho_{0.05}Yb_{0.45}$ particles were observed using SEM/EDS (JSM-5600, JEOL, Japan). The PL spectra were recorded using a spectrophotometer (Perkin Elmer LS55, UK) at room temperature. Raman spectroscopy measurements were performed using a LabRam Aramis (Horiba Jobin-Yvon, France). The 514.5 nm line of an Ar ion laser was used as the excitation source and the power on the samples was kept at 0.5 mW.

RESULTS AND DISCUSSION

Fig. 1 shows the X-ray diffraction patterns of the (a) JCPDS 40-0466 data of $KLa(MoO_4)_2$, the synthesized (b) $KLa(WO_4)_2$, (c) $KLa_{0.8}(WO_4)_2$:$Er_{0.2}$, (d) $KLa_{0.7}(WO_4)_2$:$Er_{0.1}Yb_{0.2}$ and (e) $KLa_{0.5}(WO_4)_2$:$Er_{0.05}Yb_{0.45}$ particles. The crystal structure of $KLa(WO_4)_2$ is not present in the JCPDS data. However, the diffraction patterns of the products can be mostly consistent with the standard data of scheelite structured $KLa(MoO_4)_2$ (JCPDS 40-0466). The $KLa(WO_4)_2$ with a tetragonal phase (space group: $I4_{1/a}$) had a scheelite-type crystal structure with lattice parameters of a = b = 5.4336 Å and c = 12.0866 Å[4]. Impurity phases were detected at 14.5°, 28°, 31.5° and 34° in Fig. 1d and e. The foreign reflexes are marked with an asterisk in Fig. 1e when the doping concentration of Ho^{3+}/Yb^{3+} is 0.02/0.18 mol %. A similar impurity phase was also observed in the case of Er^{3+}/Yb^{3+} doped $CaMoO_4$ phosphor when the doping concentration of Er^{3+}/Yb^{3+} is 0.02/0.18 mol %[21]. The foreign reflexes marked with an asterisk in Fig. 1d and 1e compared to the Fig. 1a and 1b can be ascribed to the fact that La^{3+}, Ho^{3+} and Yb^{3+} ions are well substituted in the tetragonal-phase $KLa(WO_4)_2$ of the Scheelite-type structure and form a new phase induced by the disorder of the $[WO_4]^{2-}$ groups. Post heat-treatment plays an important role in a well-defined crystallized morphology. To achieve a well-defined crystalline morphology, $KLa(WO_4)_2$, $KLa_{0.8}(WO_4)_2$:$Er_{0.2}$, $KLa_{0.7}(WO_4)_2$:$Er_{0.1}Yb_{0.2}$ and $KLa_{0.5}(WO_4)_2$:$Er_{0.05}Yb_{0.45}$ phases need to be heat treated at 900 °C for 16 h. It is assumed that the doping amount of Ho^{3+}/Yb^{3+} has a great effect on the crystalline cell volume of the $KLa(WO_4)_2$, because of the different ionic sizes and energy band gaps. This means that the obtained samples possess a tetragonal-phase after partial substitution of La^{3+} by Ho^{3+} and Yb^{3+} ions and the ions are effectively doped into crystal lattices of the $KLa(WO_4)_2$ phase due to the similar radii of La^{3+}, Ho^{3+} and Yb^{3+}.

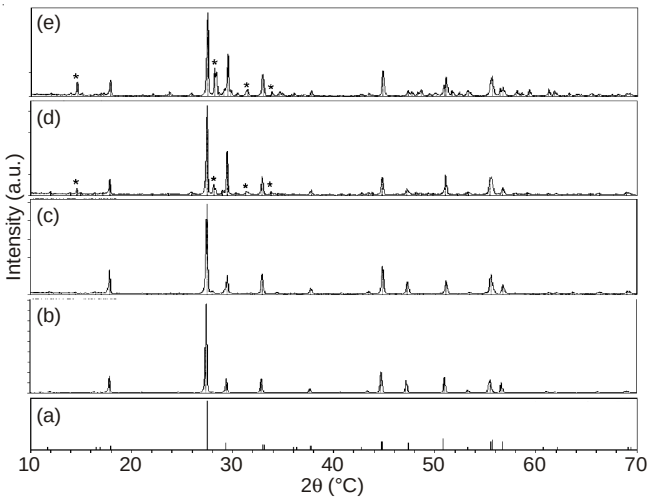

Fig. 1. X-ray diffraction patterns of the (a) JCPDS 40-0488 data of $KLa(MoO_4)_2$, the synthesized (b) $KLa(WO_4)_2$, (c) $KLa_{0.8}(WO_4)_2$:$Ho_{0.2}$, (d) $KLa_{0.7}(WO_4)_2$:$Ho_{0.1}Yb_{0.2}$, and (e) $KLa_{0.5}(WO_4)_2$:$Ho_{0.05}Yb_{0.45}$ particles

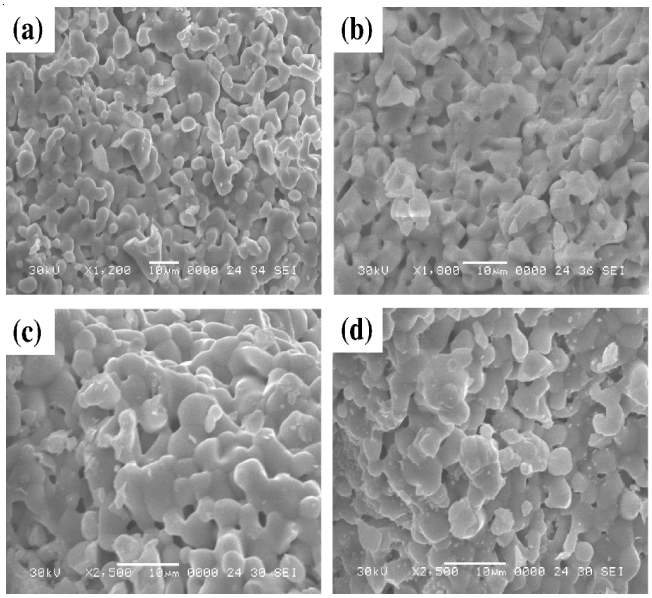

Fig. 2. Scanning electron microscopy images of the synthesized (a) $KLa(WO_4)_2$, (b) $KLa_{0.8}(WO_4)_2$:$Ho_{0.2}$, (c) $KLa_{0.7}(WO_4)_2$:$Ho_{0.1}Yb_{0.2}$, and (d) $KLa_{0.5}(WO_4)_2$:$Ho_{0.05}Yb_{0.45}$ particles

Fig. 2 shows SEM images of the synthesized (a) $KLa(WO_4)_2$, (b) $KLa_{0.8}(WO_4)_2$:$Ho_{0.2}$, (c) $KLa_{0.7}(WO_4)_2$:$Ho_{0.1}Yb_{0.2}$ and (d) $KLa_{0.5}(WO_4)_2$:$Ho_{0.05}Yb_{0.45}$ particles. The as-synthesized samples are well crystallized with a fine and homogeneous morphology and particle size of 2-5 μm. The sample of (a) $KLa(WO_4)_2$ shows a fine and homogeneous morphology. The samples of (b) $KLa_{0.8}(WO_4)_2$:$Ho_{0.2}$, (c) $KLa_{0.7}(WO_4)_2$:$Ho_{0.1}Yb_{0.2}$ and (d) $KLa_{0.5}(WO_4)_2$:$Ho_{0.05}Yb_{0.45}$ have some agglomerated particles compared to the sample of (a) $KLa(WO_4)_2$. It should be noted that the doping amounts for Ho^{3+} and Yb^{3+} have a great effect on the morphological features. Fig. 3 shows the Energy-dispersive X-ray spectroscopy patterns of the synthesized (a) $KLa_{0.8}(WO_4)_2$:$Ho_{0.2}$ and (b) $KLa_{0.5}(WO_4)_2$:$Ho_{0.05}Yb_{0.45}$ particles and quantitative compositions of (c) $KLa_{0.8}(WO_4)_2$:$Ho_{0.2}$ and (d) $KLa_{0.5}(WO_4)_2$:$Ho_{0.05}Yb_{0.45}$ particles. The EDS pattern shows that the (a) $KLa_{0.8}(WO_4)_2$:$Ho_{0.2}$ and (b) $KLa_{0.5}(WO_4)_2$:$Ho_{0.05}Yb_{0.45}$ particles are composed of K, La, W, O and Ho for $KGd_{0.8}(WO_4)_2$:$Ho_{0.2}$ and K, La, W, O, Ho and Yb for $KLa_{0.5}(WO_4)_2$:$Ho_{0.05}Yb_{0.45}$ particles. The quantitative compositions of (c) and (d) are in good relation with nominal compositions of the particles. The relation of K, La, W, O, Ho and Yb components exhibit that $KLa_{0.8}(WO_4)_2$:$Ho_{0.2}$ and $KLa_{0.5}(WO_4)_2$:

(a)

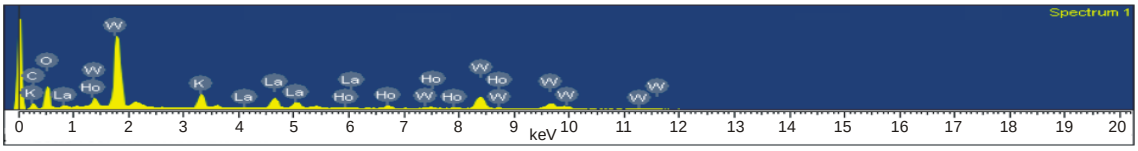

(b)

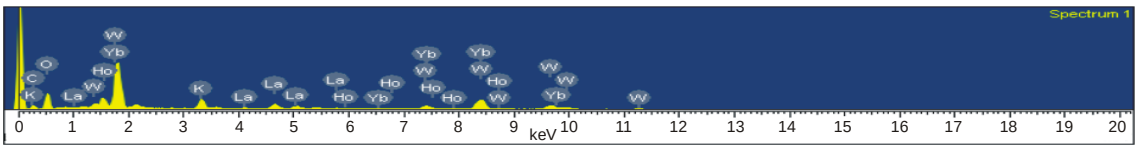

(c)

Spectrum	In stats.	C	O	K	K	Ho	W	Total
Spectrum 1	Yes	13.08	31.56	3.95	10.33	4.68	36.40	100.00
Spectrum 2	Yes	12.98	32.46	3.96	9.99	4.38	36.23	100.00
Spectrum 3	Yes	12.12	32.76	3.98	10.38	4.59	36.18	100.00
Spectrum 4	Yes	4.92	33.87	4.54	11.35	4.60	40.72	100.00
Mean		10.77	32.66	4.11	10.51	4.56	37.38	100.004
Std.deviation		3.93	0.95	0.29	0.59	0.13	2.23	
Max.		13.08	33.87	4.54	11.35	4.68	40.72	
Min.		4.92	31.56	3.95	9.99	4.38	36.18	

(d)

Spectrum	In stats.	C	O	K	La	Ho	Yb	Yb	Total
Spectrum 1	Yes	13.62	31.26	3.75	6.43	0.60	9.25	35.09	100.00
Spectrum 2	Yes	9.33	31.87	3.85	6.99	0.48	9.60	37.89	100.00
Spectrum 3	Yes	11.35	31.44	3.63	6.31	1.15	9.36	36.75	100.00
Spectrum 4	Yes	11.40	32.43	3.83	6.54	0.63	8.70	36.46	100.00
Mean		11.43	31.75	3.76	6.57	0.72	9.23	36.55	100.004
Std.deviation		1.75	0.52	0.10	0.29	0.30	0.38	1.15	
Max.		13.62	32.43	3.85	6.99	1.15	9.60	37.89	
Min.		9.33	31.26	3.63	6.31	0.48	8.70	35.09	

Fig. 3. Energy-dispersive X-ray spectroscopy patterns of the synthesized (a) $KLa_{0.8}(WO_4)_2$:$Ho_{0.2}$ and (b) $KLa_{0.5}(WO_4)_2$:$Ho_{0.05}Yb_{0.45}$ particles, and quantitative compositions of (c) $KLa_{0.8}(WO_4)_2$:$Ho_{0.2}$ and (d) $KLa_{0.5}(WO_4)_2$:$Ho_{0.05}Yb_{0.45}$ particles

$Ho_{0.05}Yb_{0.45}$ particles can be successfully synthesized using the cyclic microwave-assisted sol-gel process. The cyclic microwave-assisted sol-gel process of double tungstates provides the energy to synthesize the bulk of the material uniformly, so that fine particles with controlled morphology can be fabricated in a short time period. The method is a cost-effective way to provide highly homogeneous products and is easy to scale-up, it is a viable alternative for the rapid synthesis of upconversion particles.

Fig. 4 shows the upconversion photoluminescence emission spectra of the as-prepared (a) $KLa(WO_4)_2$, (b) $KLa_{0.8}(WO_4)_2$:$Ho_{0.2}$, (c) $KLa_{0.7}(WO_4)_2$:$Ho_{0.1}Yb_{0.2}$ and (d) $KLa_{0.5}(WO_4)_2Ho_{0.05}Yb_{0.45}$ particles excited under 980 nm at room temperature. The upconversion intensities of (c) $KLa_{0.7}(WO_4)_2$:$Ho_{0.1}Yb_{0.2}$ and (d) $KLa_{0.5}(WO_4)_2Ho_{0.05}Yb_{0.45}$ particles exhibited a strong 550 nm emission band in the green region and a very strong 655 nm emission band in the red region. The strong 550 nm emission band in the green region correspond to the $^5S_2/^5F_4 \rightarrow {}^5I_8$ transition, while the very strong emission 655 nm band in 5 the red region corresponds to the $^5F_5 \rightarrow {}^5I_8$ transferred to the activator where radiation can be emitted. The Ho^{3+} ion activator is the luminescence center for these upconversion particles and the sensitizer enhances the upconversion luminescence efficiency.

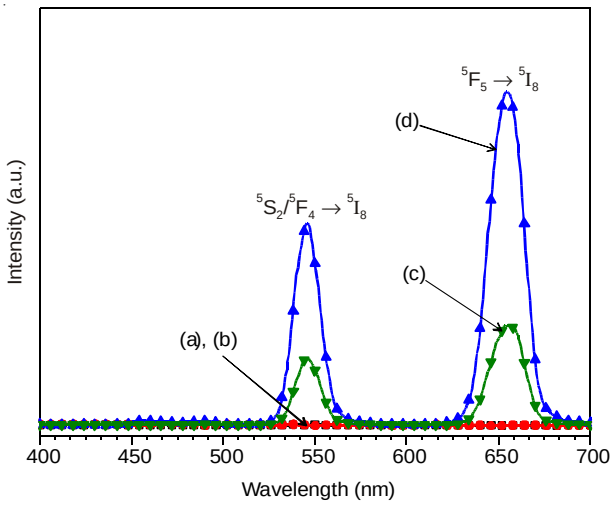

Fig. 4. Upconversion photoluminescence emission spectra of (a) $KLa(WO_4)_2$, (b) $KLa_{0.8}(WO_4)_2$:$Ho_{0.2}$, (c) $KLa_{0.7}(WO_4)_2$:$Ho_{0.1}Yb_{0.2}$ and (d) $KLa_{0.5}(WO_4)_2Ho_{0.05}Yb_{0.45}$ particles excited under 980 nm at room temperature

Fig. 5 shows the Raman spectra of the synthesized (a) $KLa(WO_4)_2$(KLW), (b) $KLa_{0.8}(WO_4)_2$:$Ho_{0.2}$ (KLW:Ho), (c) $KLa_{0.7}(WO_4)_2$:$Ho_{0.1}Yb_{0.2}$(KLW:HoYb) and (d) $KLa_{0.5}(WO_4)_2$:$Ho_{0.05}Yb_{0.45}$ (KLW:HoYb#) particles excited by the 514.5 nm line of an Ar ion laser at 0.5 mW. The internal modes for the (a) $KLa(WO_4)_2$(KLW) particles were detected at 334, 370, 816 and 932 cm^{-1}. The well-resolved sharp peaks for the $KLa(WO_4)_2$ particles indicate a high crystallinity state of the synthesized particles. The internal vibration mode frequencies are dependent on the lattice parameters and the degree of the partially covalent bond between the cation and molecular ionic group $[WO_4]^{2-}$. The Raman spectra of the (b) $KLa_{0.8}(WO_4)_2$:$Ho_{0.2}$(KLW:Ho), (c) $KLa_{0.7}(WO_4)_2$:$Ho_{0.1}Yb_{0.2}$(KLW:HoYb) and (d) $KLa_{0.5}(WO_4)_2$:$Ho_{0.05}Yb_{0.45}$ (KLW:HoYb#) particles indicate

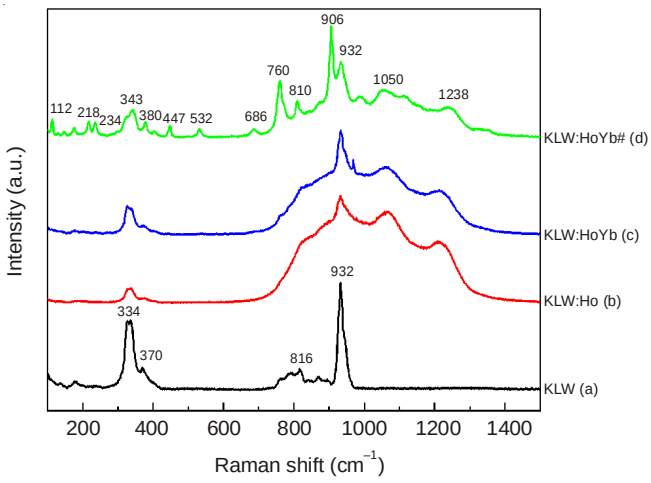

Fig. 5. Raman spectra of the synthesized (a) $KLa(WO_4)_2$(KLW), (b) $KLa_{0.8}(WO_4)_2$:$Ho_{0.2}$ (KLW:Ho), (c) $KLa_{0.7}(WO_4)_2$:$Ho_{0.1}Yb_{0.2}$(KLW: HoYb) and (d) $KLa_{0.5}(WO_4)_2$:$Ho_{0.05}Yb_{0.45}$ (KLW:HoYb#) particles excited by the 514.5 nm line of an Ar ion laser at 0.5 mW

the domination of strong peaks at higher frequencies (686, 760, 906, 1050 and 1238 cm^{-1}) and weak peaks at lower frequencies (218, 234, 447 and 532 cm^{-1}). The Raman spectra of (b) $KLa_{0.8}(WO_4)_2$:$Ho_{0.2}$ (KLW:Ho), (c) $KLa_{0.7}(WO_4)_2$: $Ho_{0.1}Yb_{0.2}$(KLW:HoYb) and (d) $KLa_{0.5}(WO_4)_2$:$Ho_{0.05}Yb_{0.45}$ (KLW: HoYb#) particles prove that the doping ions can influence the structure of the host materials. The combination of a heavy metal cation and the large inter-ionic distance for Ho^{3+} and Yb^{3+} substitutions in La^{3+} sites in the lattice result in a low probability of upconversion and phonon-splitting relaxation in $KLa_{1-x}(WO_4)_2$ crystals. It may be that these very strong and strange effects are generated by the disorder of the $[WO_4]^{2-}$ groups with the incorporation of the Ho^{3+} and Yb^{3+} elements into the crystal lattice or by a new phase formation.

Conclusion

The double tungstate $KLa_{1-x}(WO_4)_2$:Ho^{3+}/Yb^{3+} phosphors with doping concentrations of Ho^{3+} and Yb^{3+} ($x = Ho^{3+} + Yb^{3+}$, $Ho^{3+} = 0.05$, 0.1, 0.2 and $Yb^{3+} = 0.2$, 0.45) were successfully synthesized *via* the cyclic microwave-assisted sol-gel route. Well-crystallized particles formed after heat-treatment at 900 °C for 16 h showed a fine and homogeneous morphology with particle sizes of 2-5 μm. Under excitation at 980 nm, the upconversion intensities of $KLa_{0.7}(WO_4)_2$:$Ho_{0.1}Yb_{0.2}$ and $KLa_{0.5}(WO_4)_2Ho_{0.05}Yb_{0.45}$ particles exhibited a strong 550 nm emission band in the green region and a very strong 655 nm emission band in the red region, which were assigned to the $^4S_2/^5F_4 \rightarrow {}^5I_8$ and $^5F_5 \rightarrow {}^5I_8$ transitions, respectively. The upconversion intensity of $KLa_{0.5}(WO_4)_2Ho_{0.05}Yb_{0.45}$ particles was much higher than that of the $KLa_{0.7}(WO_4)_2$:$Ho_{0.1}Yb_{0.2}$ particles. The Raman spectra of the $KLa_{0.8}(WO_4)_2$:$Ho_{0.2}$, $KLa_{0.7}(WO_4)_2$: $Ho_{0.1}Yb_{0.2}$ and $KLa_{0.5}(WO_4)_2$:$Ho_{0.05}Yb_{0.45}$ particles indicated the domination of strong peaks at higher frequencies at higher frequencies (686, 760, 906, 1050 and 1238 cm^{-1}) and weak peaks at lower frequencies (218, 234, 447 and 532 cm^{-1}) induced by the disorder of the $[WO_4]^{2-}$ groups with the incorporation of the Ho^{3+} and Yb^{3+} elements into the crystal lattice or by a new phase formation.

ACKNOWLEDGEMENTS

This study was supported by the Basic Science Research Program through the National Research Foundation of Korea (NRF) funded the Ministry of Science, ICT & Future Planning (2014-046024).

REFERENCES

1. M. Wang, G. Abbineni, A. Clevenger, C. Mao and S. Xu, *Nanomedicine*, **7**, 710 (2011).
2. Y.J. Chen, H.M. Zhu, Y.F. Lin, X.H. Gong, Z.D. Luo and Y.D. Huang, *Opt. Mater*., **35**, 1422 (2013).
3. M. Lin, Y. Zhao, S.Q. Wang, M. Liu, Z.F. Duan, Y.M. Chen, F. Li, F. Xu and T.J. Lu, *Bio. Adv*, **30**, 1551 (2012).
4. L. Li, L. Liu, W. Zi, H. Yu, S. Gan, G. Ji, H. Zou and X. Xu, *J. Lumin*., **143**, 14 (2013).
5. C. Ming, F. Song and L. Yan, *Opt. Commun*., **286**, 217 (2013).
6. N. Xue, X. Fan, Z. Wang and M. Wang, *J. Phys. Chem. Solids*, **69**, 1891 (2008).
7. Z. Shan, D. Chen, Y. Yu, P. Huang, F. Weng, H. Lin and Y. Wang, *Mater. Res. Bull*., **45**, 1017 (2010).
8. W. Liu, J. Sun, X. Li, J. Zhang, Y. Tian, S. Fu, H. Zhong, T. Liu, L. Cheng, H. Zhong, H. Xia, B. Dong, R. Hua, X. Zhang and B. Chen, *Opt. Mater*., **35**, 1487 (2013).
9. W. Xu, H. Zhao, Y. Li, L. Zheng, Z. Zhang and W. Cao, *Sens. Actuators B*, **188**, 1096 (2013).
10. H. Du, Y. Lan, Z. Xia and J. Sun, *J. Rare Earths*, **28**, 697 (2010).
11. X. Liu, W. Xiang, F. Chen, W. Zhang and Z. Hu, *Mater. Res. Bull*., **47**, 3417 (2012).
12. X. Liu, W. Xiang, F. Chen, Z. Hu and W. Zhang, *Mater. Res. Bull*., **48**, 281 (2013).
13. X. Yu, Y. Qin, M. Gao, L. Duan, Z. Jiang, L. Gou, P. Zhao and Z. Li, *J. Lumin*., **153**, 1 (2014).
14. X. Yu, M. Gao, J. Li, L. Duan, N. Cao, Z. Jiang, A. Hao, P. Zhao and J. Fan, *J. Lumin*., **154**, 111 (2014).
15. J. Gu, Y. Zhu, H. Li, S. Xiong, X. Zhang, X. Wang, X. Liu and Y. Qian, *Solid State Sci*., **12**, 1192 (2010).
16. D. Thangaraju, A. Durairajan, D. Balaji and S. Moorthy Babu, *Opt. Mater*., **35**, 753 (2013).
17. J. Gu, Y. Zhu, H. Li, X. Zhang and Y. Qian, *J. Solid State Chem*., **183**, 497 (2010).
18. P. Pazik, A. Zych and W. Strek, *Mater. Chem. Phys*., **115**, 536 (2009).
19. A. Durairajan, D. Thangaraju, D. Balaji and S.M. Babu, *Opt. Mater*., **35**, 740 (2013).
20. Z. Lu and T. Wanjun, *Ceram. Int*., **38**, 837 (2012).
21. C.S. Lim, *Mater. Res. Bull*., **47**, 4220 (2012).